Diagnosis of neuroendocrine tumours by retrospective image fusion: is there a benefit?

H. Amthauer[1], J. Ruf[1], M. Böhmig[2], E. Lopez-Hänninen[1], T. Rohlfing[4], K-D. Wernecke[5], U. Plöckinger[2], M. Gutberlet[1], A.-J. Lemke[1], T. Steinmüller[3], B. Wiedenmann[2], R. Felix[1]

[1] Klinik für Strahlenheilkunde, Campus Virchow-Klinikum, Charité-Universitätsmedizin Berlin, Berlin, Germany
[2] Klinik für Hepatologie, Gastroenterologie, Endokrinologie und Stoffwechsel, Campus Virchow-Klinikum, Charité-Universitätsmedizin Berlin, Germany
[3] Klinik für Allgemein- und Transplantationschirurgie, Campus Virchow-Klinikum, Charité-Universitätsmedizin Berlin, Germany
[4] Image Guidance Laboratories, Department of Neurosurgery, Stanford University, USA
[5] Institut für Medizinische Biometrie, Campus Virchow-Klinikum, Charité-Universitätsmedizin Berlin, Germany

Received: 6 May 2003 / Accepted: 7 October 2003 / Published online: 3 December 2003

Abstract. This study evaluated the use of image fusion in the preoperative staging of neuroendocrine tumors (NET) of the pancreas and the gastrointestinal tract (GIT). Thirty-eight patients suffering from a metastasized NET with location of the primary in the pancreas (*n*=15) or the GIT (*n*=23) were examined by somatostatin receptor scintigraphy (SRS) and computed tomography (CT). Consecutive image registration and fusion were performed using custom-built software integrated in AVS/Express (Advanced Visual Systems, Waltham, MA, USA). Registration was performed by a voxel-based algorithm based on normalized mutual information. Image fusion was feasible in 36/38 patients. A total of 87 foci were assigned to anatomical regions (e.g. gut, pancreas, liver, lymph node or others) by two independent observers in both SRS and SRS/CT fusion images. The assignments used a binary ranking system (1="definite", 0="not definite"). These results were then retrospectively compared to the classification of the foci, based on postoperative histology or clinical follow-up. Imaging by SRS allowed a definite anatomical assignment in 57% (50/87) and 61% (53/87) of all lesions in the case of observers A and B, respectively. Image fusion improved the topographic assignment to 91% (79/87) and to 93% (81/87). The number classified as "definite" by both observers increased from 54% (47/87) to 86% (77/87). The increase in definite assignments was highly significant for both observers (P<0.0001 for each). In the case of foci classified as liver metastases, image fusion allowed improved assignment to the corresponding liver segment from 45% (18/40) to 98% (39/40) and from 58% (23/40) to 100% (40/40) by observers A and B, respectively. Furthermore, the improved assignment of foci classified as lesions by image fusion was relevant for therapy in 7/36 patients (19%). Therefore, the image fusion technique presented herein appears to be a very useful method for clinical routine.

Keywords: Neuroendocrine tumors – Somatostatin receptor scintigraphy – Computed tomography – Image registration – Image fusion

Eur J Nucl Med Mol Imaging (2004) 31:342–348
DOI 10.1007/s00259-003-1379-7

H. Amthauer (✉)
Klinik für Strahlenheilkunde, Campus Virchow-Klinikum,
Charité-Universitätsmedizin Berlin, Augustenburger Platz 1,
13353 Berlin, Germany
e-mail: h.amthauer@charite.de
Tel.: +49-30-450557013, Fax: +49-30-450557987

Introduction

Both somatostatin receptor scintigraphy (SRS) and computed tomography (CT) are well-established imaging procedures for the diagnosis of neuroendocrine tumours [1, 2, 3]. The detection of increased somatostatin receptor expression as a correlate for neuroendocrine tumour tissue allows very sensitive and specific detection of primary tumours, recurrent disease or metastases. However, an exact anatomical assignment is not always possible, even if single-photon emission tomography (SPET) imaging is used [4]. This is especially true in the abdominal region, where reliable assignment of pancreatic foci and their differentiation from neighbouring lymph nodes or the exact assignment of a focus to a liver segment is crucial for interventional therapeutic approaches (surgical or non-surgical). CT, on the other hand, offers detailed anatomical information on the region examined, especially when arterial and venous contrast medium phases are included [5].

The use of more than one imaging modality may provide substantial informational benefit. Techniques for the composition of two (or more) images range from simple mental integration (i.e. simultaneous visual analysis of both examinations) to various computer-assisted approaches commonly referred to as "image fusion". The latter methods require the definition of a single common coordinate system for all images so that anatomically corresponding points have the same coordinates. Transformation of the images into this coordinate system is commonly referred to as "registration". The co-registered images can easily be presented as a combined or "fused" image of both modalities by a variety of visualization methods (e.g. alternating pixels, semi-transparent overlays).

The aim of this study was to evaluate the clinical value of retrospective image fusion with regard to the detection of (metastatic) neuroendocrine tumours of the gastrointestinal tract and the pancreas.

Materials and methods

Thirty-eight patients (23 male, 15 female; age range 36–83 years, mean 55 years) diagnosed with a metastasized tumour of the gastrointestinal tract (n=23) or the pancreas (n=15) were included in this study. Histology of the primary had been obtained by resection (n=32), laparotomy (n=3) and needle biopsy (n=3).

Somatostatin receptor scintigraphy and computed tomography. Image fusion was based on image data from the corresponding SPET and CT examinations of each patient. Acquisition of SRS images included whole-body scans obtained 4, 24 and 48 h after the intravenous injection of 180–200 MBq indium-111 pentetreotide (OctreoScan, Tyco Healthcare, Petten, The Netherlands) with a double-head gamma camera (Helix, GE Medical Systems, Solingen, Germany). Furthermore, SPET of the abdominal area and/or thorax was performed 24 and 48 h after injection using a three-head gamma camera (Multispect 3, Siemens, Erlangen, Germany). Image acquisition and reconstructions were performed as recommended by Krenning et al. [3].

Native and contrast-enhanced spiral CT (Somatom Plus 4, Siemens, Erlangen, Germany) was obtained. Native scan parameters were 10 mm slice thickness, 10 mm/s table speed and 10 mm reconstruction interval. The examination was repeated in the arterial phase after the intravenous application of 100 ml contrast medium (Ultravist 370, Schering AG, Berlin, Germany) with a start delay of 18 s at a flow rate of 4 ml/s, a slice thickness of 5 mm, a table speed of 5 mm/s and an increment of 3 mm. In the final abdominal scan, the venous phase was documented after 70 s; the slice thickness was 5 mm, the table speed was 5 mm/s and the increment was 5 mm. In every patient, both CT scan and scintigraphy were performed within an interval shorter than 14 days.

Registration and image fusion. All image data were transferred in DICOM format to an SGI O2 workstation (Silicon Graphics, Mountain View, CA, USA) via our clinic-wide intranet. Registration of CT and SPET data and consecutive image visualization were performed using a custom-built software package implemented in AVS/Express 5.0 (Advanced Visual Systems, Waltham, MA, USA). Clinical applications for this registration technique have already been published elsewhere [6, 7].

Registration of medical images can in general be achieved either by prospective (e.g. stereotactic frames, fiducial markers) or retrospective techniques (e.g. manual co-registration or automatic methods based on surface or voxel intensity information) [8, 9]. In comparison to the invasive "gold standard" of stereotactic frames, co-registration of CT and SPET data by voxel-based algorithms seems most promising [10] among the non-invasive retrospective methods. In general, voxel-based registration of any two images involves finding the parameters of a coordinate transformation between them that optimize a certain measure of mutual image similarity.

For our present study, the coordinate transformation was a 3-D rigid-body transformation with six degrees of freedom (three translations and three rotations). This transformation was determined in a two-step process. As the first step, a very coarse initial registration was performed manually according to internal landmarks (e.g. kidneys) [11], adjusting the translation and rotation parameters in all three dimensions in order to achieve a close enough match between the two sets of images to ensure robust operation of the subsequent automatic algorithm. While this was not strictly required by our registration algorithm, this step, in our experience, helps to prevent failed registrations that can be caused, for example, by different image overlap or gross initial misregistration.

In the second registration step, our independent implementation of voxel-based image registration software [12] found the optimum rigid-body transformation using multi-resolution optimization of the normalized mutual information image similarity metric [13]. The previously defined manual transformation served as an initial estimate for the automatic method. Additional use of volume clipping greatly reduced computation time, and coincidence thresholding improved performance by suppression of background noise in SPET data [14].

Validation of image fusion. Retrospective voxel-based algorithms for image registration have proved to be a useful and feasible approach to image registration [10]. Furthermore, when applied to co-registration of functional and morphological imaging modalities, the results achieved using our implementation of a voxel-based registration algorithm were found to be highly accurate. This was validated by participation of our group in the "Retrospective Registration Evaluation Project" (RREP) administered by the group of J.M. Fitzpatrick at the Department of Computer Science at Vanderbilt University (Nashville, TN, USA). In this project, participants download patient image data via the Internet, apply to it their respective registration techniques and return the results for evaluation. The project organizers then compare the reported transformations to (undisclosed) gold standard transformations that were determined using bone-implanted markers.

The registration software used to obtain the results presented in this paper was validated using data from the aforementioned project [10] and consistently achieved sub-voxel registration accuracy [15]. In addition to producing highly accurate registrations, our software is extremely computationally efficient and can, for example, complete a rigid registration in less than 50 s on a current PC with a 3-GHz Pentium4 CPU (Intel, Santa Clara, CA, USA) with hyperthreading.

Evaluation of SRS scintigraphy and SRS/CT image fusion. In SRS scintigraphy, only foci within the reach of an abdominal CT scan were subject to the further evaluation process. Furthermore, hepatic lesions in patients with multiple (>4) or diffuse liver metastases on SRS scintigraphy were not subject to evaluation.

All areas with increased tracer uptake were topographically assigned in both SRS- and fused SRS/CT images by two independent nuclear medicine physicists. The categories were as follows: gut, pancreas, liver, lymph node or others (i.e. spleen, bone metastases or physiological gut uptake). Furthermore, in the case of foci assigned to the liver, hepatic lesions were attributed to the corresponding anatomical segment according to Couinaud's classification [16].

The assignment of a given SRS focus to an anatomical correlate consisted of a binary ranking system (1="definite", 0="not definite").

Verification of findings. All patients were subject to a follow-up (minimum 2 years, mean 2.8 years) consisting of clinical findings, laboratory parameters (Cg A, 5-HIAA), imaging modalities (CT, MRI, SRS, ultrasound) and in some cases resection of lesions. The classification of lesions according to clinical follow-up or histopathology served as the gold standard to which the results of SRS and SRS/CT image fusion were compared using the same categories as mentioned above.

For the classification of liver metastases, again Couinaud's classification was used.

Statistical analysis. The results of the assignments by each observer before and after image fusion were evaluated using the (exact) Mantel-Haenszel test. Two-factorial non-parametric analysis of longitudinal data was performed for the proof of differences between the observers (1st factor) and the methods (2nd factor: no fusion versus fusion), as well as for interactions between observers and methods [17]. A P value <0.05 was considered significant. Calculations were carried out with SPSS 10.0 statistical software (SPSS Inc., Chicago, IL, USA) and SAS, Release 8.2 (SAS Institute Inc., Cary, NC, USA).

Results

Assignment of lesions to anatomical regions

All image fusion results were subject to visual plausibility control. Image fusion data of 2/38 patients (5%) were excluded from further analysis, as they did not pass plausibility control due to gross variations in the position of abdominal organs.

In the remaining 36 patients, SRS showed a total of 87 lesions. Table 1 lists their distribution according to clinical follow-up or histopathology.

The overall number of definite focal assignments by SRS alone was 57% (50/87) for observer A and 61% (53/87) for observer B (Table 2). The attribution of foci to the liver achieved values of 98% (39/40) and 100% (40/40), respectively. Foci classified as pancreatic lesions were attributed in 62% (8/13) and 47% (7/13) of all cases, respectively. The assignment of foci to the gut attained values of 29% (2/7) and 43% (3/7), respectively. In the category "others", definite assignments of 10% (1/10) and 30% (3/10), respectively, were observed. The assignment was poorest for mesenteric lymph nodes: 0% (0/17) and 6% (1/17), respectively.

Based on SRS/CT image fusion, definite assignments (Table 2) were made by observer A in 91% (79/87) and by observer B in 93% (81/87).

Image fusion increased the already high number of definite attributions as hepatic lesions to 100% (40/40) each. Furthermore, all (13/13) pancreatic lesions were now correctly classified by both observers. The greatest improvement due to image fusion was seen for the classification of abdominal foci as mesenteric lymph nodes. Their assignment was "definite" in 82% (14/17) and 94% (16/17), respectively. Moderate improvements were observed for the categories "gut" [71% (5/7) and 71% (5/7), respectively] and "others" [60% (6/10) and 70% (7/10), respectively]. The overall improvement was highly significant for both observer A (P<0.0001) and observer B (P<0.0001) using the exact Mantel-Haenszel test.

As Table 2 shows, there was an increase of foci classified as "definite" by both observers from 54% (47/87) to 86% (77/87) while the number of foci that could not be definitely classified by either observer dropped from

Table 2. Results of topographical assignments of all foci (n=87) by both observers according to SRS and image fusion

		Observer A		
		Definite	Not definite	Total
Observer B	Definite	47 (77)	6 (4)	53 (81)
	Not definite	3 (2)	31 (4)	34 (6)
	Total	50 (79)	37 (8)	87 (87)

The number of assignments for SRS/CT image fusion are shown in parentheses

Table 1. Anatomical assignment of SRS foci (n=87) according to clinical follow-up and histology

	Gut	Pancreas	Mesenteric LN	Liver (segments)								Others[a]
				I	II	III	IV	V	VI	VII	VIII	
Foci	7 (6)	13 (5)	17 (9)	0	2 (2)	0	11 (3)	2	10 (4)	7 (3)	8 (3)	10 (3)

Numbers in parentheses indicate foci verified by histopathology

[a] Spleen (n=2), abdominal wall (n=1), gastric wall (n=1), bone metastases (n=3), physiological gut uptake (n=2) and bile accumulation (n=1)

Table 3. Results of topographical assignments of liver foci (n=40) by both observers according to SRS and image fusion

		Observer A		
		Definite	Not definite	Total
Observer B	Definite	14 (39)	9 (1)	23 (40)
	Not definite	4 (0)	13 (0)	17 (0)
	Total	18 (39)	37 (1)	40 (40)

The number of assignments for SRS/CT image fusion are shown in parentheses

36% (31/87) to 5% (4/87). Furthermore, the percentage of discrepant observer results dropped from 10% (9/87) to 7% (6/87). According to two-factorial non-parametric analysis of longitudinal data (first factor: observer; second factor: method, i.e. no fusion vs fusion), there were no significant differences between the observers (in the mean of the methods: P=0.19500) and no interactions between observers and methods (P=0.79733), but highly significant differences between the methods (in the mean of the observers: P<0.0001).

Segmental assignment of liver foci

Table 1 shows the segmental assignment of 40 foci classified as hepatic lesions according to follow-up or postoperative histopathology. Segmental assignment of liver foci (n=40) based on SRS yielded definite assignments in 45% (18/40) for observer A and 58% (23/40) for observer B. The highest number of definite assignments was observed in case of segment VI: 80% (8/10) and 90% (9/10), respectively. The other foci were assigned as follows: segment IV, 45% (5/11) and 73% (8/11); segment V, 50% (1/2) and 0% (0/2); segment VII, 14% (1/7) and 14% (1/7); segment II, 50% (1/2) and 100% (2/2); and segment VIII, 25% (2/8) and 38% (3/8). There were no hepatic foci assigned to segments I and III.

The use of image fusion allowed definite segmental assignment of all hepatic lesions (40/40) in the case of observer B. Observer A assigned 98% (39/40) of all foci correctly, misclassifying a segment VIII focus as an extrahepatic lesion.

After image fusion, the number of hepatic foci classified as "definite" by both observers increased from 39% (14/40) to 98% (39/40). Consequently, the number of discrepant observer results (Table 3) was reduced from 31% (13/40) to 3% (1/40). Again, non-parametric multivariate analysis revealed no significant differences (P=0.10169) or interactions (P=0.28419) between the observers.

Changes relevant for therapy due to improved assignment of foci

In about one-fifth of all patients (7/36), the more precise localization of 14/87 (16%) foci was relevant for therapy. In four cases, solitary liver metastases were enucleated. One patient with unilobular metastases underwent atypical hepatic resection. Additionally, a formerly unknown ileal primary was removed in one patient and another underwent resection of the pancreas tail as well as splenectomy after the verification of splenic infiltration. Postoperative histopathology revealed neuroendocrine tumour tissue in all resected tissue samples.

One of these patients developed a hepatic recurrence 41 months after enucleation of liver metastases. The other six patients were followed-up clinically and by imaging procedures for a period of 24–60 months: in this group no relapse was observed.

Discussion

Neuroendocrine tumours are not only classified according to their functionality, i.e. hormone or neuropeptide hypersecretion, but also according to the localization of the primary. In addition, the extent of metastatic spread is relevant for further diagnostic procedures, consecutive therapy and disease prognosis [18, 19].

In cases of locally confined disease, surgery with curative intent results in a better prognosis compared to that in patients with tumours with regional or distant metastases [20, 21]. Even in the case of hepatic metastases, enucleations, segmental resections or hemihepatectomies can be performed if the appropriate segments are known. Palliative surgery, on the other hand, allows a reduction of tumour burden or the prevention of intestinal blockage [22, 23].

Information on tumour localization and the extent of tumour spread is not only important for primary diagnosis but also crucial for the detection of recurrent disease, where the differentiation between postinterventional fibrosis and recurrence is often difficult. In this setting, functional imaging by SRS is of great importance for the detection of neuroendocrine tumour tissue. Depending on the expressed receptor subtype [24] and the localization of the primary, sensitivities of up to 97% can be achieved [4, 25]. Although tumours smaller than 1 cm may evade detection owing to the low spatial resolution of SPET [26], this technique offers the advantage of performing a whole-body scan. Nevertheless, the exact anatomical localization of foci detected by both planar and SPET imaging remains difficult, as the high percentage (36%) of foci classified as "not definite" by both observers shows.

The anatomical information is greater in morphological imaging. However, whereas the detection of liver metastases by spiral CT achieves a sensitivity of about

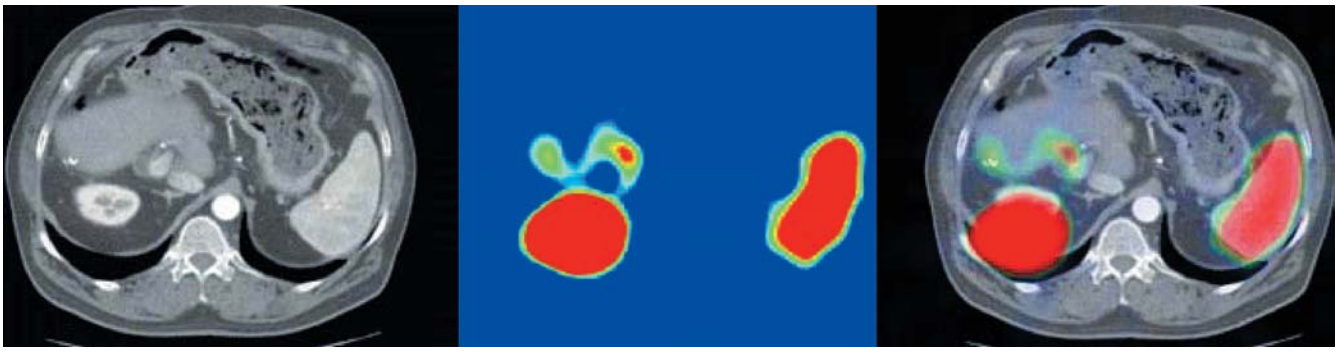

Fig. 1. Original and fused images from a 62-year-old male patient after resection of the pancreatic primary, right-sided hemihepatectomy and enucleation of liver metastases. The CT scan is shown on the *left*, the corresponding SPET image in the *centre* and the fused image on the *right*. The current SRS-SPET showed a focus suspected to be a hepatic lesion. For further clarification of the localization, image fusion was performed. However, as physiological accumulation in the right kidney was partially projected into the thorax according to the corresponding CT scan, this registration was considered to be invalid for evaluation and the patient was excluded from the study. Alterations of the patient's breathing pattern and the resulting changes in diaphragmatic excursions or different positioning of the patient were considered as possible reasons for this unsuccessful image fusion

78%, the examination is often less reliable for the detection of gastrointestinal primaries [27].

As neither modality can sufficiently fulfill the requirements demanded for the optimal planning of novel interventional techniques or multimodal therapy concepts, the combination of the two examinations might be the answer to these problems [28]. While the clinical use of mental image fusion (i.e. the correlation of image data by the human brain) is widespread, its accuracy is limited [9]. Therefore, computer-based fusion of images, or more precisely, registration of corresponding sets of data, remains desirable. Various approaches to image registration and fusion have been extensively reviewed by Maintz and Viergever [8]. Prospective techniques based on stereotactic frames or external fiducial markers have been shown to be very useful and reliable; however, preparation of the patients in the pre-acquisition phase is often time consuming [9, 29, 30] and sometimes even requires invasive measures (stereotactic frames or bone-implanted markers). However, the latter might only be tolerable for patients with locally restricted pathologies (e.g. brain tumours), where the frame system can be used for diagnostic purposes and subsequent therapy.

In comparison with the relatively rigid skull-brain system, the abdominal region is more prone to motion artefacts. First of all, the identical positioning of the patient in each examination is more difficult. External (skin-placed) markers as well surface-based retrospective techniques appear to be less suitable for the fusion of abdominal images where the localization of the abdominal wall between two examinations can differ greatly owing to breathing excursions [9, 31]. Furthermore, changes in anatomy between two scans due to excursions of the abdominal wall or diaphragm as well as bowel movement and degree of filling can influence the accuracy of abdominal image registration. Unfortunately, these inherent "systemic errors" also apply to voxel-based approaches, which have proven to be highly accurate in rigid body settings [10]. Therefore more sophisticated non-rigid registration methods (see [32] for a survey of the field) have yet to become applicable to images from multiple modalities, and especially low-resolution images such as those provided by SPET or positron emission tomography (PET). Another promising solution seems to be almost simultaneous co-registration by CT/SPET or CT/PET hybrid systems [28]. However, as these systems cannot yet be considered standard equipment, the above-mentioned various registration attempts will still play a role in clinical routine. The presented voxel-based approach by maximization of mutual information has been shown to generate accuracy substantially below the image voxel sizes in rigid-body settings [10, 13], and clinical experience with fusion PET and CT data by the same method [6, 7] suggests its usefulness even for the regions subject to motion artefacts, such as the abdomen.

Although the drop-out rate due to positioning artefacts was low in our patients (2/38), it has to be emphasized that with any image fusion technique, supervision of results and control of plausibility remain crucial (Fig. 1).

As our data show, computer-assisted fusion of image data according to the above-mentioned method, while less than perfect, not only significantly improved the anatomical assignment of lesions detected by SRS for each observer, but also reduced the number of discrepant observer assignments. The same was true for the assignments of the liver foci to the corresponding segment. Furthermore, our image fusion technique seemed to improve the localization of tumour recurrence and the differentiation between nodal and extranodal tumour manifestation (Fig. 2).

Of course, not all of these more accurate assignments resulted in an alteration in the course of therapy. However, our retrospective image fusion approach resulted in a change of therapeutic strategy in about one-fifth of all

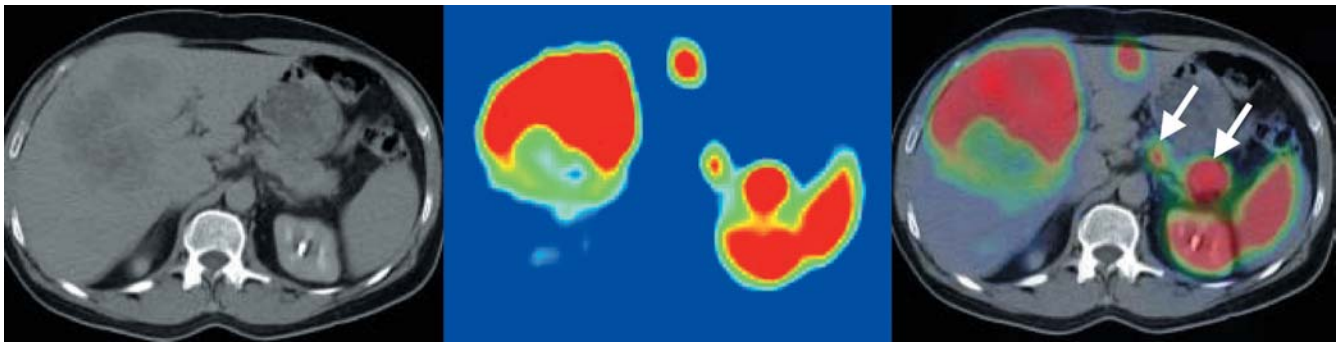

Fig. 2. Original and fused images from a 59-year-old patient with hepatic metastases of an NET of the pancreas. The CT scan is shown on the *left*, the corresponding SPET image in the *centre* and the fused image on the *right*. Aside from the hepatic metastases that were detected by both examinations, image fusion revealed a bifocal tumour of the pancreas (corpus and tail, see *arrows*). Without co-registration, the smaller tumour in the corpus would have been misjudged as a lymph node metastasis

patients, which is in concordance with the results of other studies investigating the use of image fusion for the topographical assignment of SRS foci [28, 31]. Especially in the case of hepatic foci, the presented image fusion approach was beneficial, as it allowed resection or enucleation of liver metastases with curative intent in five patients. These observations conform to those previously made at our institution using the same registration technique on a different tumour entity in the case of PET studies [6].

Conclusion

In summary, the retrospective image fusion of SRS and spiral CT is a feasible method for the integration of two imaging modalities (functional and morphological, respectively) in a single set of images. The study demonstrated that image fusion by the presented technique was a reliable and accurate tool for the diagnosis of neuroendocrine gastroenteropancreatic tumours in clinical routine. Furthermore, in comparison to the analysis of SPET images alone, fused images proved to add substantial information for the topographic assignment of SRS foci and had an impact on consecutive treatment strategies in approximately one-fifth of all patients.

Acknowledgements. This study was supported by Deutsche Forschungsgemeinschaft as part of the project Graduiertenkolleg 331: "Temperaturabhängige Effekte in Therapie und Diagnostik" (Grant No. GRK331–1/97). T.R. was supported by the National Science Foundation (USA) under Grant No. EIA-0104114.

References

1. Debray MP, Geoffroy O, Laissy JP, Lebtahi R, Silbermann-Hoffman O, Henry-Feugeas MC, Cadiot G, Mignon M, Schouman-Claeys E. Imaging appearances of metastases from neuroendocrine tumours of the pancreas. Br J Radiol 2001; 74:1065–1070.
2. Shi W, Johnston CF, Buchanan KD, Ferguson WR, Laird JD, Crothers JG, McIlrath EM. Localization of neuroendocrine tumours with [^{111}In]DTPA-octreotide scintigraphy (Octreoscan): a comparative study with CT and MR imaging. QJM 1998; 91(4):295–301.
3. Krenning EP, Kwekkeboom DJ, Bakker WH, et al. Somatostatin receptor scintigraphy with [^{111}In-DTPA-D-Phe1]- and [^{123}I-Tyr3]-octreotide: the Rotterdam experience with more than 1000 patients. Eur J Nucl Med 1993; 20:716–731.
4. Slooter GD, Mearadji A, Breeman WA, Marquet RL, de Jong M, Krenning EP, van Eijck CH. Somatostatin receptor imaging, therapy and new strategies in patients with neuroendocrine tumours. Br J Surg. 2001; 88:31–40.
5. Ricke J, Klose KJ, Mignon M, Oberg K, Wiedenmann B. Standardisation of imaging in neuroendocrine tumours: results of a European delphi process. Eur J Radiol 2001; 37:8–17.
6. Hosten N, Kreissig R, Puls R, Amthauer H, Beier J, Rohlfing T, Stroszczynski C, Herbel A, Lemke AJ, Felix R. Fusion von CT- und PET-Daten: Methoden und klinische Bedeutung am Beispiel der Planung der laserinduzierten Thermotherapie von Lebermetastasen. Rofo Fortschr Geb Rontgenstr Neuen Bildgeb Verfahr 2000; 172:630–635.
7. Hosten N, Lemke AJ, Wiedenmann B, Böhmig M, Rosewicz S. Combined imaging techniques for pancreatic cancer. Lancet 2000; 356:909–910.
8. Maintz JB, Viergever MA. A survey of medical image registration. Med Image Anal 1998; 2:1–36.
9. Israel O, Keidar Z, Iosilevsky G, Bettman L, Sachs J, Frenkel A. The fusion of anatomic and physiologic imaging in the management of patients with cancer. Semin Nucl Med 2001; 31:191–205.
10. West J, Fitzpatrick JM, Wang MY, et al. Comparison and evaluation of retrospective intermodality brain image registration techniques. J Comput Assist Tomogr 1997; 21:554–566.
11. Wagenknecht G, Kaiser HJ, Büll U. Multimodale Integration, Korrelation und Fusion von Morphologie und Funktion: Methodik und erste klinische Anwendungen. Rofo Fortschr Geb Rontgenstr Neuen Bildgeb Verfahr. 1999; 170:416–426.
12. Studholme C, Hill DLG, Hawkes DJ. Automated three-dimensional registration of magnetic resonance and positron emission tomography brain images by multiresolution optimisation of voxel similarity measures. Med Phys 1997; 24:25–35.

13. Studholme C, Hill DLG, Hawkes DJ. An overlap invariant entropy measure of 3D medical image alignment. Pattern Recognition 1999; 32:71–86.
14. Rohlfing T, Beier J. Improving reliability and performance of voxel-based registration by coincidence thresholding and volume clipping. In: Hawkes DJ, Hill DLG, Gaston R, eds. Proceedings of medical image understanding and analysis. London: Kings College; 1999:165–168.
15. Rohlfing T. Multimodale Datenfusion für die bildgesteuerte Neurochirurgie und Strahlentherapie. PhD thesis, Technische Unversität Berlin, 2000.
16. Couinaud C. Le foie. Etudes anatomiques et chirurgicales. Paris: Masson, 1957.
17. Brunner E, Domhof S, Langer F. Nonparametric analysis of longitudinal data in factorial experiments. Hoboken, NJ: Wiley, 2002.
18. Kulke MH, Mayer RJ. Carcinoid tumors. N Engl J Med. 1999; 340:858–868.
19. Wiedenmann B, Jensen RT, Mignon M, Modlin CI, Skogseid B, Doherty G, Oberg K. Preoperative diagnosis and surgical management of neuroendocrine gastroenteropancreatic tumors: general recommendations by a consensus workshop. World J Surg 1998; 3:309–318.
20. Modlin IM, Sandor A. An analysis of 8305 cases of carcinoid tumors. Cancer 1997; 79:813–829.
21. Hofler H, Stier A, Schusdziarra V, Siewert JR. Klassifikation der neuroendokrinen Tumoren des Gastrointestinaltrakts und des Pankreas und ihre therapeutische Relevanz. Chirurg 1997; 68:107–115.
22. Pascher A, Steinmuller T, Radke C, Hosten N, Wiedenmann B, Neuhaus P, Bechstein WO. Primary and secondary hepatic manifestation of neuroendocrine tumors. Langenbecks Arch Surg 2000; 385:265–270.
23. Schmidbauer S, Ladurner R, Juckstock H, Trupka AW, Mussack T, Hallfeldt KK. Die operative und adjuvante Therapie neuroendokriner Tumoren des Gastrointestinaltrakts und ihrer Metastasen. Chirurg 2001; 72:945–952.
24. Patel YC. Somatostatin and its receptor family. Front Neuroendocrinol 1999; 20:157–198.
25. Anthony LB, Martin W, Delbeke D, Sandler M. Somatostatin receptor imaging: predictive and prognostic considerations. Digestion 1996; 57 Suppl 1:50–53.
26. Kisker O, Weinel RJ, Geks J, Zacara F, Joseph K, Rothmund M. Value of somatostatin receptor scintigraphy for preoperative localization of carcinoids. World J Surg 1996; 20:162–167.
27. Sugimoto E, Lorelius LE, Eriksson B, Oberg K. Midgut carcinoid tumours. CT appearance. Acta Radiol 1995; 36:367–371.
28. Even-Sapir E, Keidar Z, Sachs J, Engel A, Bettman L, Gaitini D, Guralnik L, Werbin N, Iosilevsky G, Israel O. The new technology of combined transmission and emission tomography in evaluation of endocrine neoplasms. J Nucl Med 2001; 42:998–1004.
29. Weber DA, Ivanovic M. Correlative image registration. Semin Nucl Med 1994; 24:311–323.
30. Mongioj V, Brusa A, Loi G, Pignoli E, Gramaglia A, Scorsetti M, Bombardieri E, Marchesini R. Accuracy evaluation of fusion of CT, MR, and SPECT images using commercially available software packages (SRS PLATO and IFS). Int J Radiat Oncol Biol Phys 1999; 43:227–234.
31. Perault C, Schvartz C, Wampach H, Liehn JC, Delisle MJ. Thoracic and abdominal SPECT-CT image fusion without external markers in endocrine carcinomas. The Group of Thyroid Tumoral Pathology of Champagne-Ardenne. J Nucl Med. 1997; 38:1234–1242.
32. Lester H, Arridge SR. A survey of non-linear medical image registration. Pattern Recognition 1999; 32:129–149.